Available online at www.sciencedirect.com
ScienceDirect
Journal of Sound and Vibration 318 (2008) 1109–1118
JOURNAL OF SOUND AND VIBRATION
www.elsevier.com/locate/jsvi

Study on a new nonlinear parametric excitation equation: Stability and bifurcation

Chen Si-yu*, Tang Jin-yuan

Key Laboratory of Modern Complex Equipment Design and Extreme Manufacturing (Central South University), Ministry of Education, Hunan Changsha 410083, China

Received 20 November 2007; received in revised form 31 January 2008; accepted 27 April 2008
Handling Editor: L.G. Tham
Available online 16 June 2008

Anstract

The parameter stability and global bifurcations of a strong nonlinear system with parametric excitation and external excitations are investigated in detail. Using the method of Multiple scales, the nonlinear system is transformed to the averaged equation. The parameter stability of solution in the case of principal parametric resonance is developed. Based on the averaged equation, the continuation algorithm is utilized to analyze the detailed bifurcation scenario as the parameter f_0 is varied. The results indicate that there exist two limit points and neutral saddle points. Finally, a series of branching points were obtained by changing the parameters f_0 and ρ.

1. Introduction

Parametrically excited vibrations have been extensively applied to engineering systems [1], such as the vibration of machines, dynamically buckled motions of elastic structures, the roiling motions of ships, the motions of rockets and satellites, dynamic vibration of gear pairs system, etc. These physical systems may be modeled as a system of nonlinear dynamics with parametric excitation and external excitation [1].

In the past two decades, research on nonlinear dynamics with parametric excitation and external excitation has received more and more attention [2–5]. Parameter stability problem of the parametrically excited system is an important and difficult one. Furthermore, the global bifurcations and chaotic dynamics of the system are studied much less, especially in dynamic vibration of gear pairs system with time-varying stiffness and time-varying damping coefficient and external excitation [6].

In 1997, Esmailzadeh and Nakhaie-Jazar [7] found that there exit necessary and sufficient conditions for the existence of at least one periodic solution for the Mathieu–Duffing equation. Natsiavas et al. [8,9] investigated a Mathieu–Duffing oscillator under constant external load. They revealed that the oscillator examined may exhibit strong (first-order) resonance for two ranges of the forcing frequency. The first one occurs around the

*Corresponding author. Tel./fax: +86 731 2656545.
E-mail address: csyd5053@yahoo.com.cn (C. Si-yu).

0022-460X/$ - see front matter
doi:10.1016/j.jsv.2008.04.055

excitation frequency, and it has an identical form with the Mathieu–Duffing oscillator under principal parametric resonance. However, unlike the Mathieu–Duffing oscillator with no constant external forcing, the system examined by Refs. [8,9] exhibited a second strong resonance, which occurs in forcing frequency ranges near the linear natural frequency. Luo [10,11] in 2003 investigated the Mathieu–Duffing oscillator with a twin-well potential, and in his work the approximate criteria for the onset and destruction of a specified, primary resonant band of the Mathieu–Duffing oscillator was developed. Ng et al. [12,13] investigated the Mathieu equation to which is added a cubic nonlinearity x^3 term using averaging method. The main objective of the above studies was to apply both analytical and numeric methodology for determining periodic steady-state motions.

On the research of local and global bifurcations of parametric excitation systems, the literature [14–18] must be mentioned. The global bifurcations and chaotic dynamics for high-dimensional nonlinear systems are very important theoretical problems in science and engineering as they can reveal the instabilities of motion and complicated dynamical behaviors.

Zhang and Yu [14] considered the dynamical properties of both local and global bifurcations for a parametrically and externally excited mechanical system. With the aid of normal form theory and the method of Multiple scales, they found that this system could exhibit the homoclinic and heteroclinic bifurcations and multiple limit cycles. Cao et al. [15] studied the global bifurcations and chaotic dynamics of a string-beam system subject to parametric and external excitations by using the method of Galerkin and Multiple scales. The theory of normal form was also used to find the explicit formulas of normal form associated with one double zero and a pair of pure imaginary eigenvalues. The bifurcation analysis indicated that the coupled system can undergo pitch and homoclinic bifurcation and the Silnikov-type single-pluse homoclinic orbit. Sofroniou and Bishop [16] investigated the effect of the symmetry breaking by comparing the control parameter space of frequency and amplitude of the forcing with its symmetric counterpart. Approximate bifurcation analysis was used to predict the new escape boundary using a harmonic balance scheme. Li et al. [17] implied that motion of the parametrically and externally excited mechanical system can jump from a lower-energy plane to a higher-energy plane, which was also associated with jumping phenomena of the amplitude-modulated oscillations.

In this paper, we will consider the control equation of gear pairs system combined with friction and time-varying stiffness following [6]:

$$\ddot{x} + \varepsilon c_0(1 + c_e \sin \omega t)\dot{x} + k_0(1 + \varepsilon k_e \sin \omega t)f(x) = f_0 + \varepsilon f_1 \sin \omega t \tag{1}$$

which is a strong nonlinear parametric excitation system, where the dots indicate differentiation with respect to time t, ε is a small parameter, c_0 is the coefficient of viscous damping, k_0 is the coefficient of stiffness, c_e, k_e and ω are respectively the amplitude and frequency of the parametric excitation, f_0 and f_1 are the amplitudes of the external excitation. The piecewise linear function of gear backlash is simplified as

$$f(x) = -x + \varepsilon m x^3 \tag{2}$$

where m is the coefficient of the nonlinear term.

In this paper, we will investigate the stability and the bifurcation of the equilibria of Eq. (1). The original system is transformed to the averaged equation by Multiple-scales method. Then, we get the parameter regions of stability and instability. The bifurcation parameters of the system are controlled to obtain two generic codim 1 bifurcations that can be detected along the equilibrium curve. Finally, the route of continuation of the codim 2 bifurcation is investigated.

2. Solutions using the Multiple-scales method

We may use the expansion procedure obtained formally by the Multiple-scales method [1,10,11,18]. The independent variable t can be extended to introduce alternative independent variables:

$$T_n = \varepsilon^n t, \quad n = 0, 1, 2 \tag{3}$$

where T_0 is fast variable, and T_1, T_2 are the slow variables. The operator can now be expressed as the derivative expansions:

$$\frac{dx}{dt} = D_0x_0 + \varepsilon(D_0x_1 + D_1x_0) + \varepsilon^2(D_0x_2 + D_1x_1 + D_2x_0) + O(\varepsilon^3) \tag{4}$$

$$\frac{d^2x}{dt^2} = D_0^2x_0 + \varepsilon(2D_0D_1x_0 + D_0^2x_1) + \varepsilon^2(D_1^2x_0 + D_0^2x_2 + 2D_0D_1x_1 + 2D_0D_2x_0) + O(\varepsilon^3) \tag{5}$$

When the nonlinearity is assumed to be of order ε, x may be represented by an expansion having the form

$$x(t,\varepsilon) = x_0(T_0,T_1,T_2) + \varepsilon x_1(T_0,T_1,T_2) + \varepsilon^2x_2(T_0,T_1,T_2) + \varepsilon^3x_3(T_0,T_1,T_2) \tag{6}$$

Then we substitute Eq. (6) into Eq. (1) and set the coefficient of each power of ε equal to zero. Each of the x_n are independent of ε, substituting Eqs. (4)–(6) into Eq. (1) and collecting terms order-by-order in ε sequence of differential equations are obtained

$$\begin{aligned} &\varepsilon^0: \quad D_0^2x_0 - k_0x_0 = f_0 \\ &\varepsilon^1: \quad D_0^2x_1 - k_0x_1 = f_1\sin\omega t - 2D_0D_1x_0 - c_0(1 + c_e\sin\omega t)D_0x_0 - (mk_0x_0^3 + k_0k_ex_0\sin\omega t) \end{aligned} \tag{7,8}$$

Let $k_0 = \omega_1^2$, to the first-order approximation, these resonant conditions are (a) principal resonance $\omega = \omega_1$, (b) superharmonic resonance $\omega = \omega_1/n$ and (c) subharmonic resonance $\omega = \omega_1/n$.

The principal resonance $\omega = \omega_1$ is the one to be analyzed in this paper. To describe quantitatively the nearness of these resonances, we introduce the detuning parameters σ as follows:

$$\omega = \omega_1 + \varepsilon\sigma \tag{9}$$

Then, we can get the solution of Eq. (7) as follows:

$$x_0 = A(T_1)\exp(i\omega_1T_0) + \bar{A}(T_1)\exp(-i\omega_1T_0) + f_0/k_0 \tag{10}$$

where $A(T_1)$ is an undetermined function of T_1 at this level of approximation, and $\bar{A}(T_1)$ is the complex conjugate of $A(T_1)$. They can be determined by imposing the solvability conditions at the next level of approximation.

According to the Multiple-scales theory, by substituting Eq. (10) into Eq. (8) and using Eq. (9), the equation is expressed in the single-DOF form:

$$D_0^2x_1 + k_0x_1 = \left(-3m\omega_1^2A^2A_1 - \frac{3mf_0^2}{\omega_1^2}A - \frac{1}{2}if_1e^{i\rho T_1} + \frac{1}{2}if_0k_1e^{i\rho T_1} - ic_0\omega_1A - iA'\omega_1\right)e^{i\omega_1T_0} + CC \tag{11}$$

Eliminating the terms that produce secular terms in Eq. (11) yields the solvability condition:

$$-3m\omega_1^2A^2A_1 - \frac{3mf_0^2}{\omega_1^2}A - \frac{1}{2}if_1e^{i\rho T_1} + \frac{1}{2}if_0k_1e^{i\rho T_1} - ic_0\omega_1A - iA'\omega_1 = 0 \tag{12}$$

In order to solve Eq. (12), we introduce the polar form

$$A = \tfrac{1}{2}a\exp(ib) \tag{13}$$

where a, b are real functions of time T_1. Substituting Eq. (13) into Eq. (12), we get

$$\begin{aligned} &-\frac{3m\omega_1^2a^3}{8}\exp(ib) - \frac{3mf_0^2a}{2\omega_1^2}\exp(ib) + \frac{1}{2}i(f_0k_1 - f_1)e^{i\rho T_1} \\ &- i\frac{c_0\omega_1a}{2}\exp(ib) - \left(\frac{1}{2}i\omega_1a'\exp(ib) - \frac{1}{2}\omega_1ab'\exp(ib)\right) = 0 \end{aligned} \tag{14}$$

Letting $e^{i(\rho T_1 - b)} = \cos(\rho T_1 - b) + i\sin(\rho T_1 - b)$ and separating the real and imaginary parts of the resulting equations yield the following set of amplitude- and phase-modulation equations:

$$\begin{cases} -\dfrac{3m\omega_1^2 a^3}{8} - \dfrac{3mf_0^2 a}{2\omega_1^2} + \frac{1}{2}\omega_1 ab' - \frac{1}{2}(f_0 k_1 - f_1)\sin(\rho T_1 - b) = 0 \\ \frac{1}{2}(f_0 k_1 - f_1)\cos(\rho T_1 - b) - \dfrac{c_0\omega_1 a}{2} - \frac{1}{2}\omega_1 a' = 0 \end{cases} \tag{15}$$

So

$$\begin{aligned} ab' &= \frac{3m\omega_1 a^3}{4} + \frac{3mf_0^2 a}{\omega_1^3} + \frac{f_0 k_1 - f_1}{\omega_1}\sin(\rho T_1 - b) \\ a' &= \frac{f_0 k_1 - f_1}{\omega_1}\cos(\rho T_1 - b) - c_0 a \end{aligned} \tag{16,17}$$

Let

$$\varphi = \rho T_1 - b \quad \text{or} \quad \frac{d\varphi}{dT_1} = \rho - \frac{db}{dT_1} \tag{18}$$

Eqs. (16) and (17) are translated to

$$\begin{aligned} a\frac{d\varphi}{dT_1} &= \rho a - \frac{3m\omega_1 a^3}{4} - \frac{3mf_0^2 a}{\omega_1^3} - \frac{f_0 k_1 - f_1}{\omega_1}\sin\varphi \\ \frac{da}{dT_1} &= \frac{f_0 k_1 - f_1}{\omega_1}\cos\varphi - c_0 a \end{aligned} \tag{19,20}$$

there are two possibilities: either trivial solutions

$$a = 0 \tag{21}$$

Or non-trivial solutions,

$$a \neq 0 \tag{22}$$

we only take the second condition into consideration. Periodic solutions of Eq. (1) correspond to the fixed points of Eqs. (19) and (20), which are obtained by setting $(d\varphi/dT_1) = 0$, $(da/dT_1) = 0$.

$$a^6 + \vartheta_1 a^4 + \vartheta_2 a^2 + \vartheta_3 = 0 \tag{23}$$

where $\lambda_i (i = 1,2,3)$ are parameters which can be represented as,

$$\begin{aligned} &\lambda_1 = 8\left(\frac{3mf_0^2}{\omega_1^3} - \rho\right)\bigg/ 3m\omega_1, \lambda_2 = \left[\left(\frac{3mf_0^2}{\omega_1^3} - \rho\right)^2 + c_0^2\right]\bigg/\left(\frac{3m\omega_1}{4}\right)^2, \\ &\lambda_3 = -\left(\frac{f_0 k_1 - f_1}{\omega_1}\right)^2\bigg/\left(\frac{3m\omega_1}{4}\right)^2 \end{aligned} \tag{24,25,26}$$

3. Stability of the solutions

In this section, we will detect the stability of the solution and get the regions of parameter stability. We also consider the Eq. (19) and (20).

$$\begin{aligned} a\frac{d\varphi}{dT_1} &= \rho a - \frac{3m\omega_1 a^3}{4} - \frac{3mf_0^2 a}{\omega_1^3} - \frac{f_0 k_1 - f_1}{\omega_1}\sin\varphi \\ \frac{da}{dT_1} &= \frac{f_0 k_1 - f_1}{\omega_1}\cos\varphi - c_0 a \end{aligned} \tag{27}$$

In the investigation of the stability of the trivial solutions, it is important to transform Eq. (27) into the Cartesian form in order to avoid dividing by a. By using the change of variables,

$$u = a\cos\varphi, \quad v = a\sin\varphi \tag{28}$$

In Eq. (27), we can obtain

$$\begin{aligned}\frac{\mathrm{d}u}{\mathrm{d}T_1} &= \frac{f_0k_1 - f_1}{\omega_1} - c_0u - \left(\rho - \frac{3mf_0^2}{\omega_1^3} - \frac{3m\omega_1}{4}(u^2+v^2)\right)v \\ \frac{\mathrm{d}v}{\mathrm{d}T_1} &= -c_0v + \left(\rho - \frac{3mf_0^2}{\omega_1^3} - \frac{3m\omega_1}{4}(u^2+v^2)\right)u\end{aligned} \tag{29,30}$$

We need to investigate the characteristic equation of the Jacobian matrix of the averaged Eqs. (29) and (30),

$$D_wf = \begin{bmatrix} -c_0 + \frac{3m\omega_1}{2}u & -\rho + \frac{3mf_0^2}{\omega_1^3} + \frac{3m\omega_1}{4}u^2 + \frac{9m\omega_1}{4}v^2 \\ \rho - \frac{3mf_0^2}{\omega_1^3} - \frac{9m\omega_1}{4}u^2 - \frac{3m\omega_1}{4}v^2 & -c_0 - \frac{3m\omega_1}{2}uv \end{bmatrix} \tag{31}$$

where

$$w = (u, v)^{\mathrm{T}} \tag{32}$$

$$f = \begin{bmatrix} \frac{f_0k_1 - f_1}{\omega_1} - c_0u - \left(\rho - \frac{3mf_0^2}{\omega_1^3} - \frac{3m\omega_1}{4}(u^2+v^2)\right)v \\ -c_0v + \left(\rho - \frac{3mf_0^2}{\omega_1^3} - \frac{3m\omega_1}{4}(u^2+v^2)\right)u \end{bmatrix} \tag{33}$$

And also the Eq. (33) can be translated,

$$f^* = \begin{bmatrix} -c_0x - \left(\rho - \frac{3mf_0^2}{\omega_1^3} - \frac{3m\omega_1}{4}\left((x+\bar{b})^2 + (y+\bar{c})^2\right)\right)y + \frac{3m\omega_1}{4}\left((x+\bar{b})^2 + (y+\bar{c})^2\right)\bar{c} \\ -c_0y + \left(\rho - \frac{3mf_0^2}{\omega_1^3} - \frac{3m\omega_1}{4}\left((x+\bar{b})^2 + (y+\bar{c})^2\right)\right)x - \frac{3m\omega_1}{4}\left((x+\bar{b})^2 + (y+\bar{c})^2\right)\bar{b} \end{bmatrix} \tag{34}$$

where $\bar{b}$, $\bar{c}$ are the roots of the following equations,

$$\begin{cases} \frac{f_0k_1 - f_1}{\omega_1} - \left(\rho - \frac{3mf_0^2}{\omega_1^3}\right)c - c_0b = 0 \\ \left(\rho - \frac{3mf_0^2}{\omega_1^3}\right)b - c_0c = 0 \end{cases} \tag{35,36}$$

The Jacobian matrix of the averaged Eqs. (35) and (36) is,

$$D_{w*}f^* = \begin{bmatrix} -c_0 + \frac{3m\omega_1}{2}(x+\bar{b})(y+\bar{c}) & -\rho + \frac{3mf_0^2}{\omega_1^3} + \frac{9m\omega_1}{4}(y+\bar{c})^2 + \frac{3m\omega_1}{4}(x+\bar{b})^2 \\ \rho - \frac{3mf_0^2}{\omega_1^3} - \frac{9m\omega_1}{4}(x+\bar{b})^2 - \frac{3m\omega_1}{4}(y+\bar{c})^2 & -c_0 - \frac{3m\omega_1}{2}(y+\bar{c})(x+\bar{b}) \end{bmatrix} \tag{37}$$

The eigenvalue equation can be obtained at $\bar{x} = \bar{y} = 0$,

$$\begin{vmatrix} \lambda + (c_0 - 2\eta\bar{b}\bar{c}) & -\mu + 3\eta\bar{c}^2 + \eta\bar{b}^2 \\ \mu - 3\eta\bar{b}^2 - \eta\bar{c}^2 & \lambda + (c_0 - 2\eta\bar{b}\bar{c}) \end{vmatrix} = 0 \tag{38}$$

where

$$2\eta = \frac{3m\omega_1}{2}, \quad \mu = \rho - \frac{3mf_0^2}{\omega_1^3}, \quad \beta = \frac{f_0k_1 - f_1}{\omega_1}, \quad \bar{b} = \frac{c_0\beta}{\mu^2 + c_0^2}, \quad \bar{c} = \frac{\mu\beta}{\mu^2 + c_0^2}$$

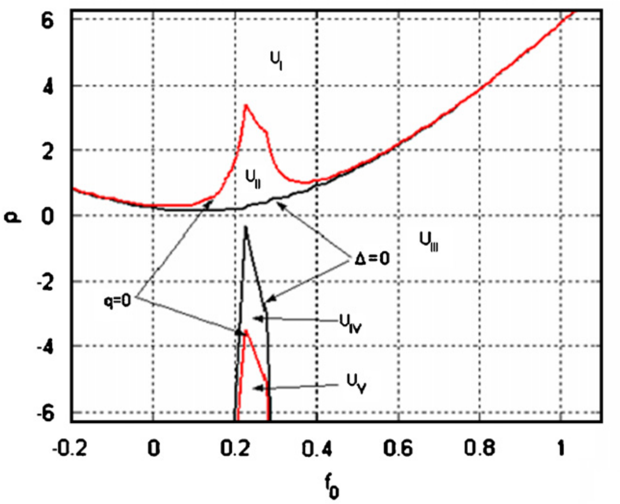

Fig. 1. Parameter stability regions: $\omega_1 = 0.5975, f_1 = 10, k_1 = 41.33, c_0 = 3.436, m = 0.3$, the red and black lines of the figure correspond to the case $q = 0$ and $\Delta = 0$.

And the eigenvalues can be depicted as,

$$\lambda_{1,2} = -\frac{1}{2}p \pm \sqrt{\Delta} \tag{39}$$

where

$$p = 2c_0,$$
$$q = c_0^2 - (4\eta\mu\bar{b}^2 + 4\eta\mu\bar{c}^2 + 6\eta^2\bar{b}^2\bar{c}^2 + \mu^2 - 3\eta^2\bar{c}^4 - 3\eta^2\bar{b}^4),$$
$$\Delta = p^2 - 4q = 4(4\eta\mu\bar{b}^2 + 4\eta\mu\bar{c}^2 + 6\eta^2\bar{b}^2\bar{c}^2 + \mu^2 - 3\eta^2\bar{c}^4 - 3\eta^2\bar{b}^4) \tag{40,41,42}$$

There are four different cases on the condition of $\Delta > 0$,

(1) with $q < 0$, the eigenvalues λ_1, λ_2 are contrary roots, and then singular point $(\bar{b}, \bar{c})$ is a saddle point, and the steady-state solution is instability.
(2) with $q > 0$, $p > 0$, $\Delta > 0$, both λ_1, λ_2 are negative roots, and the singular point $(\bar{b}, \bar{c})$ is a stable node.
(3) with $q > 0$, $p > 0$, $\Delta < 0$, λ_1, λ_2 are conjugate complex roots with $\Re(\lambda) < 0$. Hence, the singular point is a stable focus.
(4) with $q > 0$, $p > 0$, $\Delta = 0$, λ_1, λ_2 are negative double roots, the singular point is a stable critical node.

Fig. 1 illustrates the stability and instability of parameters f_0 and ρ. The corresponding parameters are chosen as $\omega_1 = 0.5975$, $f_1 = 10$, $k_1 = 41.33$, $c_0 = 3.436$, $m = 0.3$. The red and black lines of the figure correspond to the case $q = 0$and $\Delta = 0$, respectively. We can obtain five different stability regions as follows,

(1) in regions of $U_{\mathrm{I}} = \{(f_0,\rho)|q > 0,\Delta > 0\}$, $U_V = \{(f_0,\rho)|q > 0,\Delta > 0\}$, singular point $(\bar{b}, \bar{c})$ is a node point.
(2) $U_{\mathrm{II}} = \{(f_0,\rho)|q < 0,\Delta > 0\}$, $U_{\mathrm{III}} = \{(f_0,\rho)|q < 0,\Delta < 0\}$, $U_{\mathrm{IV}} = \{(f_0,\rho)|q < 0,\Delta > 0\}$, in these regions, the singular point are unstable saddle points.

4. Bifurcation and continuation

The main goal of the above section was to qualitatively characterize the nature of the stationary solution , which was approached at long times. Our next goal is to study the pattern of bifurcation that takes place as we vary the parameter f_0. This can done by studying the change in the eigenvalue of the Jacobian matrix and also following the continuation algorithm. In continuous-time systems there are two generic codim 1 bifurcations, fold and Hopf-point, that can be detected along the equilibrium curve. The equilibrium curve can also have branch points. To detect these singularities, there are three test functions,

$$\phi_1(x,f_0) = \det\begin{pmatrix} F_x \\ v^{\mathrm{T}} \end{pmatrix}, \quad \phi_2(x,f_0) = \det(2f_x(x,f_0)\Theta I_n), \quad \phi_3(x,f_0) = v_{n+1} \tag{43,44,45}$$

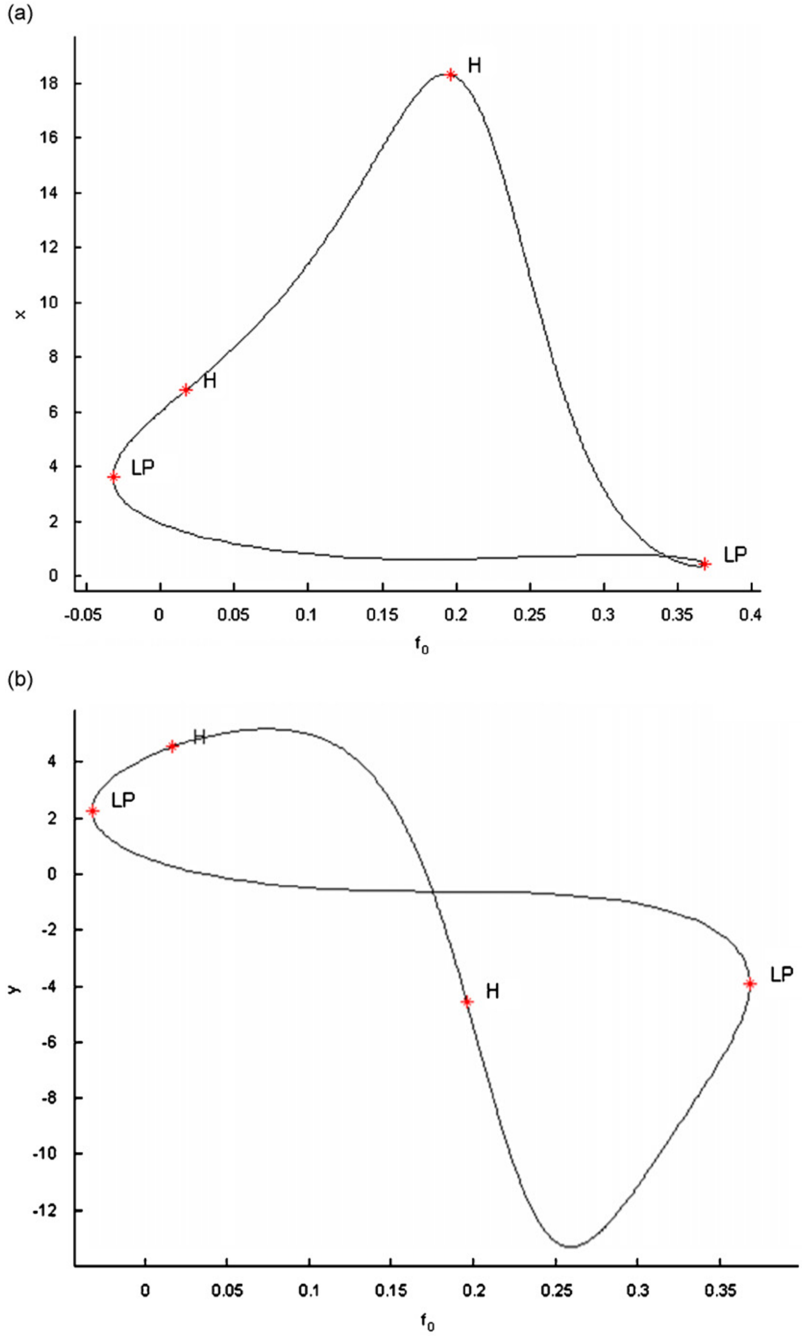

Fig. 2. Continuation curves of equilibrium with the variation of the parameter of the variables (a) x and (b) y: $\omega_1 = 0.5975$, $f_1 = 10$, $k_1 = 41.33$, $c_0 = 3.436$, $m = 0.3$.

where Θ is the bialternate matrix product. We can define the singularities, according to these test functions:

(1) Limit point (LP), also known as fold, when $\phi_3 = 0$, $\phi_1 \neq 0$,
(2) Hopf point and neutral saddles (H), when $\phi_2 = 0$,
(3) Branching point (BP), when $\phi_1 = 0$.

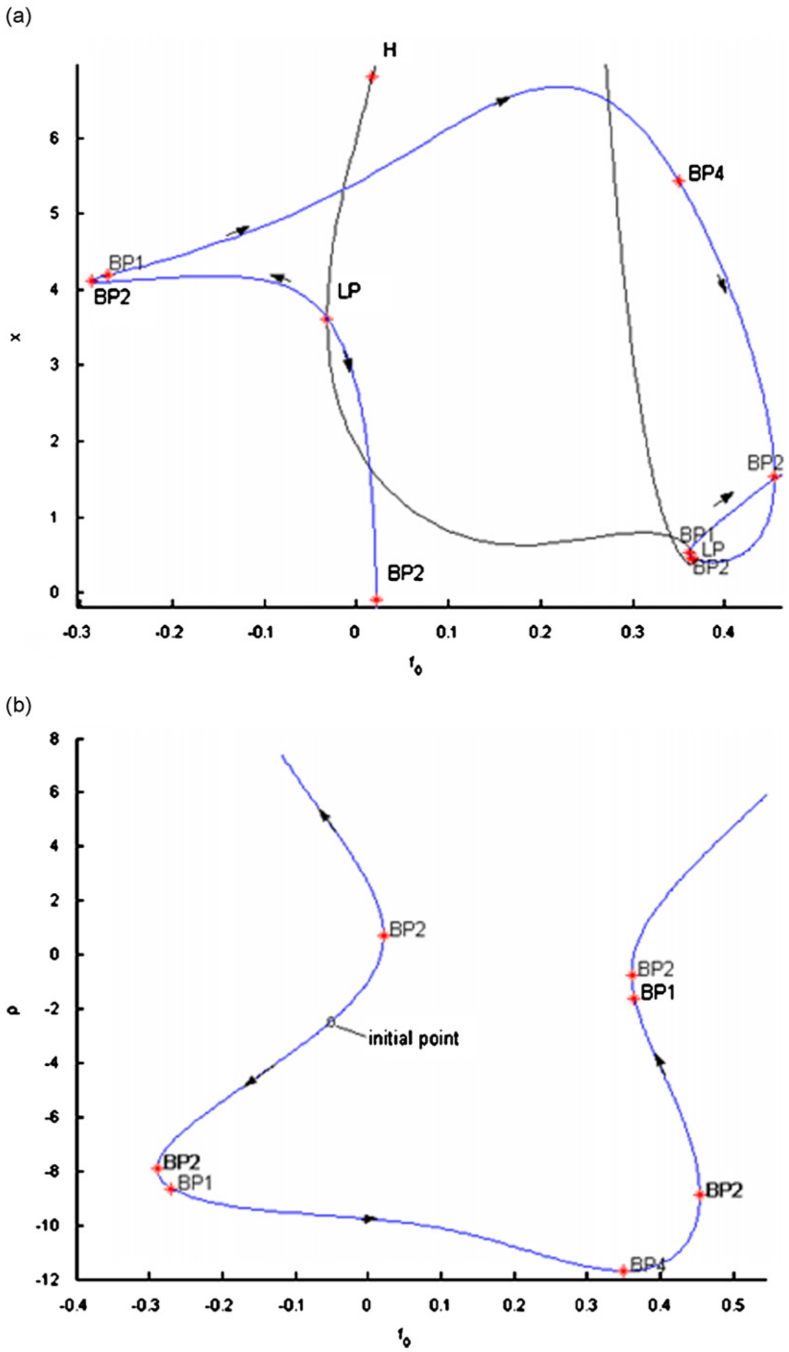

Fig. 3. Continuation curves of equilibrium with the variation of the parameters of the variables f_0 and ρ: $\omega_1 = 0.5975, f_1 = 10, k_1 = 41.33$, $c_0 = 3.436$, $m = 0.3$.

In the second case, we notice that $\phi_2 = 0$ not only at Hopf points but also at neutral saddles, and that f_x has two real eigenvalues with sum zero. In generic one-parameter ODEs, one eigenvalue $\lambda_1 = 0$ is algebraically simple at the LP-bifurcation and no other eigenvalues with $\Re(\lambda) = 0$ are present. At $f_0 = f_0{}^*$, there is a smooth one-dimensional invariant manifold W_0^c in the phase space of Eq. (37), which is called the critical center manifold at the LP-bifurcation. The curve can be locally parameterized by $u \in \mathbb{R}$ with small $|u|$. The restriction of Eq. (37) to W_0^c has the form

$$\dot{u} = au^2 + O(|u|^3) \tag{46}$$

where a is the quadratic normal form coefficient for the LP bifurcation, and can be obtained from

$$a = \frac{1}{2}\, p_1^{\mathrm{T}} f_{xx}[q_1, q_1] \tag{47}$$

where $f_x q_1 = f_x{}^{\mathrm{T}} p_1 = 0$, $p_1^{\mathrm{T}} q_1 = 1$.

To start with we consider a set of fixed point $x_0 = 0$, $y_0 = 0$, using the same parameters as above. The characteristics of the limit cycle and the general bifurcation may be explored by using the software package MATCONT [19]. This package is a collection of numerical algorithms implemented as a MATLAB toolbox for the detection, continuation and identification of limit cycles. In this package we use prediction-correction continuation algorithm based on the Moore–Penrose matrix pseudo inverse for computing the curves of equilibria, limit point (LP), Hopf bifurcation points(H) or Neutral saddle points, along with branching point(BP), etc. Fig. 2 shows the continuation curve from the equilibrium point with f_0 as the control parameter. In the figure we get two limit points (LP) and two Neutral saddle points (H).

The two limit points denoted by LP are located at $(x, y, f_0) = (0.437528, -3.932474, 0.368395)$, where the corresponding quadratic normal form coefficient is -3.057365e-001 and at $(x, y, f_0) = (3.618341, 2.262011, -0.031927)$, where the corresponding quadratic normal form coefficient is 3.576476e-001. There are also two Neutral saddle points denoted by H, which are located at $(x, y, f_0) = (18.313111, -4.552072, 0.196211)$ and $(x, y, f_0) = (6.803775, 4.547622, 0.017365)$.

We now consider the starting point to be the LP occurring at $f_0 = -0.031927$, as shown in Fig. 3. f_0 and ρ are considered as control parameters. The corresponding continuation curves of equilibrium for (f_0, x) and (f_0, ρ) are shown in Fig. 3a, b, respectively, and denoted by blue line. The arrowheads denote the continuation direction. In the Fig. 3a, the black continuation curves is the same as shown in Fig. 2a.

By changing the values of f_0 and ρ we arrived at branching points (BP2, BP1, BP4, BP2, BP1, BP2) as shown on the forward direction, and the corresponding coordinates (x, y, f_0, ρ) are (4.105790, −2.206431, −7.917460, −0.288332), (4.184944, −2.489451, −8.640557, −0.269899), (5.424375, −8.851477, −11.690066, 0.350706), (1.533801, −8.119698, −8.895372, 0.453956), (0.459540, −3.714532, −1.622045, 0.364811), (0.527386, −3.235752, −0.745466, 0.361046). In the backward direction we also get branching point at (−0.082969, 4.897345, 0.707488, 0.021201).

5. Conclusion

In above analyses we have explored the parameter stability of a strong nonlinear parametric excitation system by using the Multiple-scales method. In this way, the nonlinear system is transformed to the averaged equation and the corresponding amplitude- and phase-modulation equations are obtained. The parameter stability of solution in the case of principal parametric resonance is developed. Based on the averaged equation, the continuation algorithm is utilized to analyze the detailed bifurcation scenario as the parameter f_0 is varied. The interesting outcome are the occurrence of various kinds of bifurcation points, such as limit point and neutral saddle points, and a closed curve as the process of continuation takes place. Finally, we obtain a set of branching points by tuning both parameters f_0 and ρ.

Acknowledgments

The authors gratefully acknowledge the support of the National Science Foundation of China (NSFC) through Grants nos. 50475139, National Basic Research Program of China (2005CB724100).

References

[1] A.M. Elnaggar, A.A. Alhanadwah, Parametric excitation of subharmotion oscillations, *International Journal of Theoretical Physics* 36 (8) (1997) 1921–1940.

[2] K. Szabelski, J. Warminski, Self-excited system vibrations with parametric and external excitations, *Journal of Sound and Vibration* 187 (1995) 595–607.

[3] A. Yu Kolesov, N. Kh Rozov, Parametric excitation of high-mode oscillations for a non-linear telegraph equation, *SB MATH* 191 (8) (2000) 1147–1169.

[4] Qinglong Ma, A. Kahraman, Subharmonic resonances of a mechanical oscillator with periodically time-varying, piecewise-nonlinear stiffness, *Journal of Sound and Vibration* 294 (2006) 624–636.

[5] Gong Cheng, W. Jean Zu, A numerical study of a dry friction oscillator with parametric and external excitations, *Journal of Sound and Vibration* 287 (2005) 329–342.

[6] J.Y. Tang, et al., A improved nonlinear model of a spur gear pair system, *Engineering Mechanics* 1 (25) (2008) 217–223 (in Chinese).

[7] E. Esmailzadeh, G. Nakhaie-Jazar, Periodic solution of a Mathieu–Duffing type equation, *International Journal of Non-linear Mechanics* 5 (32) (1997) 905–912.

[8] S. Natsiavas, S. Theodossiades, Piecewise linear systems with time varying coefficient, *ASME Design Engineering Technical Conference*, Sacramento, CA, 1997.

[9] S. Natsiavas, S. Theodossiades, I. Goudas, Dynamic analysis of piecewise linear oscillators with time periodic coefficient, *International Journal of Nonlinear Mechanics* 35 (2000) 53–68.

[10] A.C.J. Lou, Chaotic motion in the generic separatrix bands of a Mathieu–Duffing oscillator with a twin-well potential, *Journal of Sound and Vibration* 3 (248) (2001) 521–532.

[11] A.C.J. Lou, Chaotic motion in the resonant separatrix bands of a Mathieu–Duffing oscillator with a twin-well potential, *Journal of Sound and Vibration* 3 (273) (2004) 653–666.

[12] L. Ng, Bifurcations in a Mathieu equation with cubic nonlinearities, *Chaos, Solitons and Fractals* (17) (2002) 173–181.

[13] L. Ng, R. Band, Bifurcations in a Mathieu equation with cubic nonlinearities, *Communications in Nonlinear Science and Numerical Simulation* 7 (2002) 107–121 (Part II).

[14] W. Zhang, P. Yu, Degenerate bifurcation analysis on a parametrically and externally excited mechanical system, *International Journal of Bifurcation Chaos* 11 (2001) 689–709.

[15] D.X. Cao, W. Zhang, Global bifurcations and chaotic dynamics for a string-beam coupled system, *Chaos, Solitons & Fractals* (2006).

[16] A. Sofroniou, S.R. Bishop, Breaking the symmetry of the parametrically excited pendulum, *Chaos, Solitons & Fractals* 28 (2006) 673–681.

[17] J. Li, et al., Analysis on bifurcations of multiple limit cycles for a parametrically and externally excited mechanical system, *Chaos, Solitons & Fractals* 31 (2007) 960–976.

[18] A.F. El-Bassiouny, On methods for continuous systems with quadratic, cubic and quantic nonlinearities, *Chaos, Solitons & Fractals* (2007).

[19] A. Dhooge, W. Govaerts, Y.A. Kuznetsov, MATCONT: A Matlab package for numerical bifurcation analysis of ODEs, *ACM Trans Math Software* 29 (2003) 141–164.